Verification of the Predicting Model and Characteristics of Dye-Based Ink Jet Printer

Takayuki Ogasahara ▲
Canon Inc., Tokyo, Japan

For analyzing color reproduction of an ink jet printer, it is important to fully understand the relationship between amounts of dye placed on the paper and resultant colors. This insight will enable one to develop a simulation that can be used to design optimum subtractive color dyes. The purpose of the present study is to verify the predicting models that can predict tristimulus values from printed dye amounts, for use in evaluating the performance of dye-based ink jet printers (IJs). In the present study, five predicting models were compared for dye-based IJ, including the Neugebauer model, the Yule–Nielsen Neugebauer model, the Kubelka–Munk model, the Cellular Neugebauer model, and the Cellular Kubelka–Munk model. Further, the comparison between a dye-based IJ and photographic color paper was studied by means of a computer simulation. This investigation was carried out from the viewpoints of the stability of selective grays for illumination metamerism and of maximizing color gamut volumes. For a dye-base IJ, the effect of ink dilution was also studied. This study is an important step toward the development of simulations for use in improving image quality for dye-based IJ.

Journal of Imaging Science and Technology 48: 130–137 (2004)

Introduction

Recently, ink jet printer technology has been advancing rapidly. Among a variety of factors controlling image quality of ink jet printers (IJs), granularity and tone reproduction have been improved considerably by ink dilution and small droplet technology. In such a situation, it will be important to increase the size of the color gamut of subtractive color dyes. Development for the optimum subtractive color dyes will rely on the full understanding of the relationship between dye amounts placed on the paper and resultant colors. In the field of photography and printing, the models used to predict reproduced tristimulus values from dye amounts include the Neugebauer model, the Yule–Nielsen Neugebauer model, and the Kubelka–Munk model.[1–4]

Recently, IJ manufacturers have used dyes to realize larger color gamuts. However, there are few studies on the maximization of color gamut from dye-based IJs. Five predicting models for dye-based IJs are compared below. In the previous study,[5–7] the optimum subtractive color dyes in a photographic color film and paper were studied by means of computer simulation for maximum stability of gray balance and color gamut. In follow-up to those studies, these two factors are compared here for controlling image quality between a dye-based IJ and a photographic color paper by using the optimum predicting model within a computer simulation. Also the effect of ink dilution has been studied about the factors of gray balance stability and color gamut.

Predicting Models

The Neugebauer model (NM)[8] has been widely used for modeling binary color printers. It is the multicolorant generalization of the Murray–Davies equation[9] that is employed here for predicting the reflectance of multicolorant mixtures in halftone printing. The Neugebauer equation is written as follows:

$$\hat{R}_\lambda(\lambda) = \sum_i p_i R_{\lambda,i}(\lambda) \tag{1}$$

where $\hat{R}_\lambda(\lambda)$ is the predicted spectral reflectance, $R_{\lambda,i}(\lambda)$ represents the measured spectral reflectance of Neugebauer primaries, and p_i is the weight applied to the i^{th} Neugebauer primary. If the dot locations for colorants are placed using a random or rotated screen,[10,11] the Demichel equation[12] is assumed to hold, and the primary set is shown below for a set of 2 colorants:

$$\begin{aligned} p_1 &= \left(1 - a_{colorant(1)}\right)\left(1 - a_{colorant(2)}\right) \\ p_2 &= a_{colorant(1)}\left(1 - a_{colorant(2)}\right) \\ p_3 &= \left(1 - a_{colorant(1)}\right)a_{colorant(2)} \\ p_i &= a_{colorant(1)}a_{colorant(2)} \end{aligned} \tag{2}$$

where $a_{colorant}$ is the area covered by primary colorant. This area can often be calculated by regression.

However there is considerable difference between the reflectance predicted by the NM and the measured re-

Original manuscript received July 11, 2003

▲ IS&T Member

Takayuki0513@aol.com

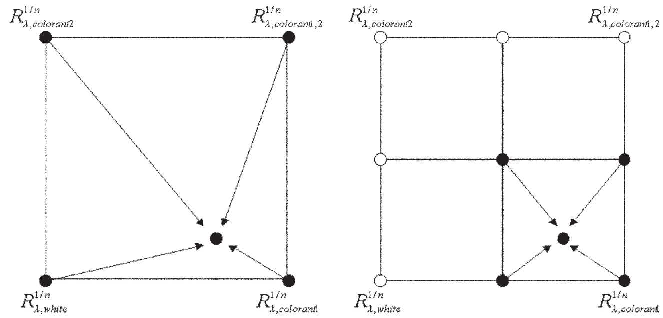

Figure 1. Illustration of two colorant model. Left side is the NM that has 4 primaries and area coverages of 0% and 100%. Right side is the CNM that has 32 = 9 primaries and area coverages of 0%, 50%, and 100%. Solid circles show the Neugebauer primaries.

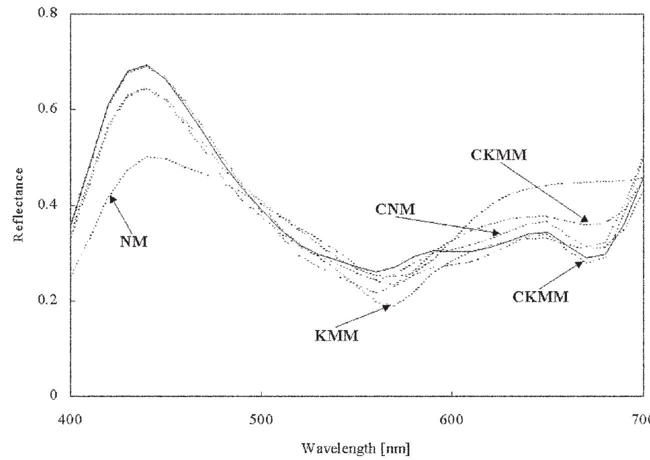

Figure 2. Predicted spectral reflectances obtained by the NM, YNNM, KMM, CNM, and CKMM (dotted lines), and measured spectral reflectance (solid line) for an example out of 486 samples.

flectance because of the effect of light scattering in the paper. Therefore Yule and Nielsen[13–15] modified the Neugebauer equation to predict results in the presence of light scattering. The Yule–Nielsen Neugebauer equation (YNNM) is written as follows:

$$\hat{R}_\lambda(\lambda) = \left(\sum_i p_i R^{1/n}_{\lambda,i,\max}(\lambda) \right)^n \quad (3)$$

where n is the Yule–Nielsen exponent. Typically n is determined through minimizing some metrics such as ΔE_{94} or spectral reflectance RMS error.

The Kubelka–Munk model (KMM),[16–19] which was developed as a series of equations useful for predicting reflectance in many types of colorant systems, is often used as an approach for translucent and opaque media. The Kubelka–Munk equation is written as follows:

$$\hat{R}_\lambda(\lambda) = \left(\sum_i p_i R^{1/n}_{\lambda,i,\max}(\lambda) \right)^n \quad (4)$$

$$k_{\lambda,i} = -0.5 \ln\left\{ R_{\lambda,i}(\lambda) / R_{\lambda,paper}(\lambda) \right\} \quad (5)$$

where $R_{\lambda,paper}$ is the spectral reflectance of the paper, c represents concentration, and k_λ defines the absorptivity of each colorant.

To better predict reflectance, the Cellular Neugebauer model (CNM)[20–22] restricts the effective area coverage used by the Neugebauer equation within narrow limits geometrically as shown in Fig. 1. From Fig. 1, we obtain:

$$a'_{eff} = \frac{a_{eff} - a_{eff,lower}}{a_{eff,upper} - a_{eff,lower}} \quad (6)$$

where a'_{eff} is normalized effective area coverage based on the upper and lower bounding area coverage of the cell. The Cellular Kubelka–Munk model (CKMM)[23] restricts the concentration used by the Kubelka–Munk equation within narrow limits geometrically, the same as the CNM.

Experimental Results

A Canon S900 was used as a dye-based IJ. In fact, the IJ employs six inks of cyan (C), magenta (M), yellow (Y), black (K), 1/6 density photo cyan (pC), and 1/6 density photo magenta (pM) and its printing resolution is 1200 × 1200 dpi. In this present study, a coated paper (Professional Photo Paper) was used. A GretagMacbeth SpectroScan spectrophotometer was used to make all the spectral measurements. The predicting models described above were used and compared among the NM, YNNM (n = 10.0), KMM, CNM (n = 10.0), and CKMM.

TABLE I. Comparison of Prediction Accuracy Among Predicting Models

	NM	YNNM	KMM	CNM	CKMM
Average ΔE_{94} D65	5.56	3.59	6.54	1.92	2.15
Standard deviation	3.28	2.13	4.39	1.42	1.69
Maximum	14.92	10.20	20.47	8.40	8.98
Minimum	0.05	0.03	0.00	0.04	0.00
Average ΔE_{94} A	5.63	3.63	6.81	1.90	2.24
RMS spectral error	0.048	0.029	0.027	0.017	0.013

Two Colorant Model Evaluation

We used 486 (81 × 6) printed samples that composed of two colorants as CM, CY, CK, MY, MK, and YK for evaluation of each predicting model. The CNM and CKMM used area coverages and concentrations of 0%, 50%, and 100%, so the set of primaries was $3^2 = 9$. As summarized in Table I, the CNM and CKMM showed better results than others by ΔE_{94} and spectral reflectance RMS error. The value of ΔE_{94} was improved about two-fold from the YNNM to the CNM and about three-fold from the KMM to the CKMM. Figure 2 shows an example reflectance and its predictions from the various models.

Three Colorant Model Evaluation

Product development requirements for a dye-based IJ in the high end photographic market are typically set at less than ΔE_{94}. Based on the results of the two colorant model evaluation as summarized in Table I, the CNM and CKMM were chosen as the best candidate models for further evaluation; ΔE_{94} and spectral reflectance RMS error were used to evaluate performance in predicting 800 random printed samples, where each was composed of three colorant combinations from C, M, Y, and K. Three sets of primaries used by the CNM and CKMM were 2^3 = 8 (0%, 100%), 3^3 = 27 (0%, 50%, 100%), and 5^3 = 125 (0%,

TABLE II. Three Colorant Prediction Accuracy of the CNM

The set of primaries	$2^3 = 8$	$3^3 = 27$	$5^3 = 125$
Average ΔE_{94} D65	6.26	1.53	1.13
Standard deviation	2.77	0.78	0.61
Maximum	13.44	5.08	3.71
Minimum	0.48	0.09	0.11
Average ΔE_{94} A	6.94	1.64	1.13
RMS spectral error	0.036	0.011	0.006

TABLE III. Three Colorant Prediction Accuracy of the CKMM

The set of primaries	$2^3 = 8$	$3^3 = 27$	$5^3 = 125$
Average ΔE_{94} D65	7.78	4.72	2.89
Standard deviation	4.30	2.74	1.54
Maximum	21.05	14.77	8.53
Minimum	0.69	0.33	0.14
Average ΔE_{94} A	8.72	5.33	3.20
RMS spectral error	0.031	0.027	0.018

TABLE IV. Four Colorant Prediction Accuracy of the CNM

The set of primaries	$2^4 = 16$	$3^4 = 81$	$5^4 = 625$
Average DE_{94} D65	6.30	2.24	1.13
Standard deviation	3.58	1.24	0.67
Maximum	16.06	6.87	3.43
Minimum	0.57	0.09	0.06
Average DE_{94} A	6.78	2.33	1.17
RMS	0.022	0.008	0.004

TABLE V. Four Colorant Prediction Accuracy of the CKMM

The set of primaries	$2^4 = 16$	$3^4 = 81$	$5^4 = 625$
Average ΔE_{94} D65	11.44	5.85	3.27
Standard deviation	4.67	3.04	2.14
Maximum	26.24	16.83	9.60
Minimum	0.75	0.46	0.07
Average ΔE_{94} A	12.11	6.19	3.49
RMS spectral error	0.019	0.016	0.012

25%, 50%, 75%, 100%). The set of 8 primaries (0%, 100%) was used within the NM and KMM.

As shown in Table II, an increase from 8 to 27 primaries for the CNM considerably improved prediction accuracy in terms of ΔE_{94} and spectral reflectance RMS error; 125 primaries resulted in the target prediction accuracy of $\Delta E_{94} \cong 1.0$. For the CKMM summarized in Table III, an increase from 8 to 125 primaries could not achieve sufficient prediction accuracy.

Four Colorant Model Evaluation

Evaluation of ΔE_{94} and spectral reflectance RMS error was used for additional 800 random printed samples where each was composed of four colorant combinations of C, M, Y, and K; three sets of primaries, $2^4 = 16$, $3^4 = 81$, and $5^4 = 625$, were used for the CNM and CKMM. For the CNM, more than 625 primaries were required to get the same prediction accuracy as the three colorant evaluation. For the CKMM, an increase from 16 primaries to 625 primaries could again not achieve sufficient prediction accuracy. See Tables IV and V.

Comparison with a Photographic Paper

Recently, image quality of IJs has been rapidly advancing, and thereby, opportunities to print pictures taken

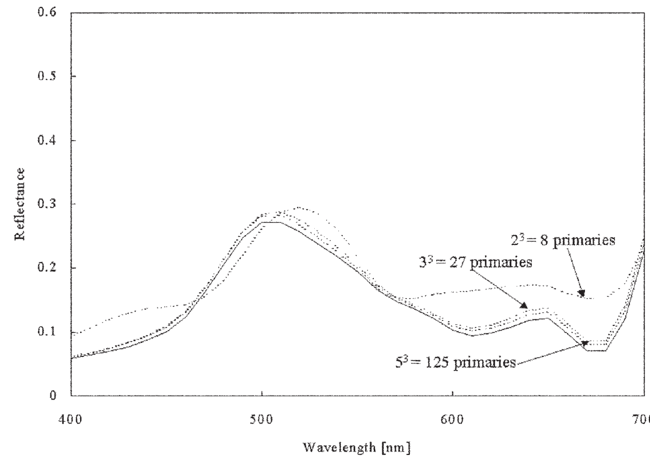

Figure 3. Predicted spectral reflectances obtained by the CNM (dotted lines), and measured spectral reflectance (solid line) for one example out of 800 samples.

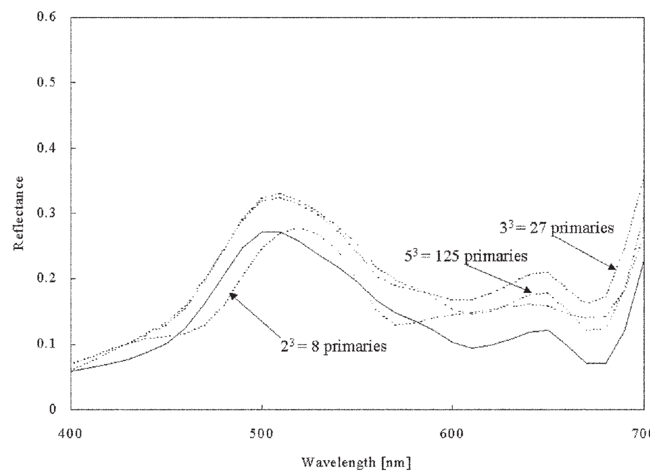

Figure 4. Predicted spectral reflectances obtained by the CKMM (dotted lines), and measured spectral reflectance (solid line) for one example out of 800 samples.

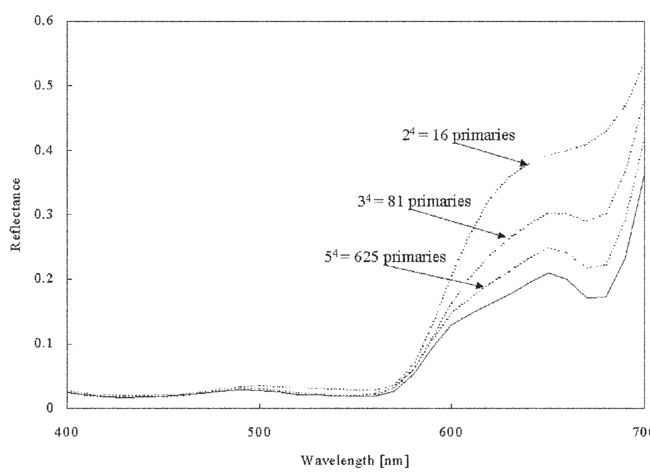

Figure 5. Predicted spectral reflectances obtained by the CNM (dotted lines), and measured spectral reflectance (solid line) for one example out of 800 samples.

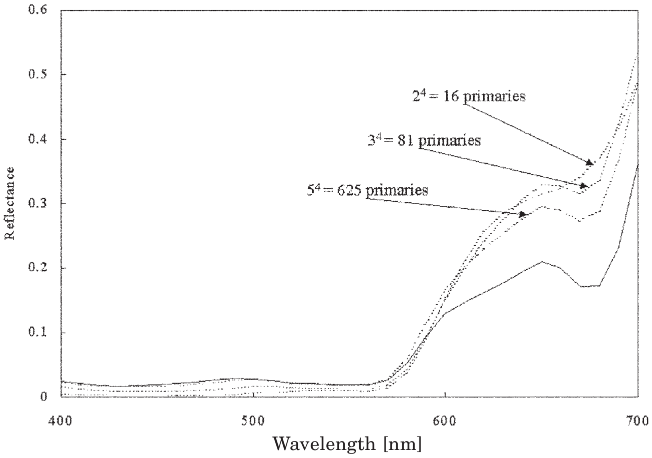

Figure 6. Predicted spectral reflectances obtained by the CKMM (dotted lines), and measured spectral reflectance (solid line) for one example out of 800 samples.

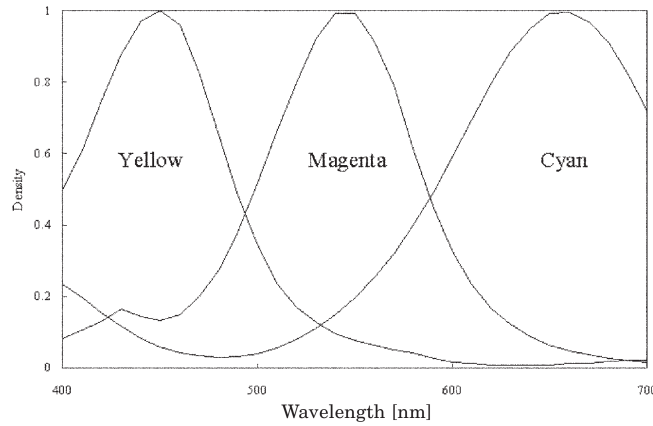

Figure 7. Spectral transmission density of C, M, and Y dyes for a photographic color paper.

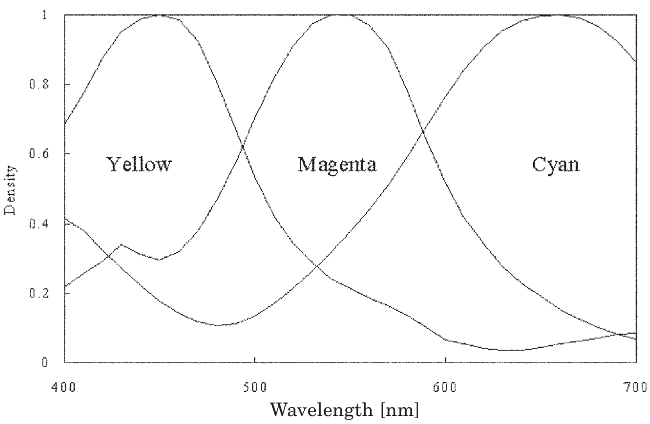

Figure 8. Spectral reflection density with surface reflection of 0.6% of C, M, and Y dyes for a photographic color paper.

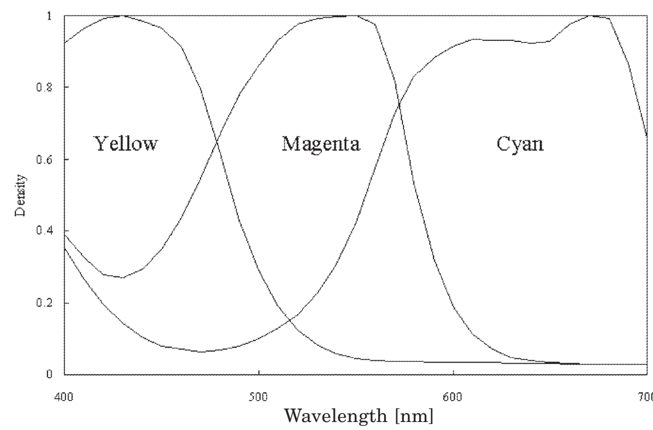

Figure 9. Spectral reflection density of C, M, and Y dyes for a dye-based IJ.

with a digital camera, using a dye-based IJ, will increase. For such a situation, two factors for controlling image quality were calculated using CIE94 under D65 and 2° observer, and comparison made between a dye-based IJ and photographic color paper.

Stability of Gray Balance

The stability of selective grays formed by a combination of C, M, and Y dyes was studied by means of computer simulation. The Newton–Raphson technique was employed to calculate grays for photographic color paper and for dye-based IJ. The photographic color paper simulation was described on the assumption that the Williams and Clapper equation[24,25] holds as shown below in Eq. (7). The dye-based IJ simulation was built from the use of the CNM with the set of primaries $5^3 = 125$.

$$R = 0.193T^{2.13}\left[\frac{1}{2R_B} - \int_0^{\pi/2} T^{2\sec\theta} r_\theta \sin\theta\cos\theta d\theta\right]^{-1} \quad (7)$$

where T = transmittance of the gelatin layer, R_B = reflectance of the paper base is taken as 0.985, θ = angle of reflection of the light from the paper base, internal Fresnel reflectance of the interface, θ, and R = reflectance when that of the paper base is taken as 1.0.

For the theoretical formula in Eq. (7), it is assumed that diffusion by the base is anosotropic. The surface reflection[26] from a coated paper for dye-based IJ obtained from measured reflection densities and Eq. (8) was 0.6%, so the surface reflection in a color paper was likewise taken as 0.6% for comparison under the same condition.

$$D' = -\log\left(10^{-d} + S\right) + \log\left(1 + S\right) \quad (8)$$

where S is the surface reflectance, D' and D are the reflection densities with and without the surface reflection. Peak transmission density of C, M, and Y dyes was taken as 4.0, and peak reflection density of C, M, and Y dyes obtained by the Williams and Clapper equation, Eq. (7) reached 2.2. The numerical integration was done with the Simpson's rule together with Newton's 3/8 rule,[27] and all code was written in C.

Typical subtractive color dyes in a photographic color paper, quoted from Ohta,[27] were used in this study. Spectral transmission density curves of C, M, and Y dyes are shown in Fig. 7 after normalizing to 1.0 peak density. Spectral reflection density curves of C, M, and Y dyes that are obtained therefrom by the Williams and Clapper equation, Eq. (7) are shown in Fig. 8 after normalizing to 1.0 peak density. Spectral reflection density curves of C, M, and Y dyes that are used by a dye-based IJ are shown in Fig. 9 after normalizing to 1.0 peak density.

TABLE VI. Index of Metamerism Illuminant A

Lightness	Dye-based IJ	Photo Color Paper
L* = 80	1.58	0.77
L* = 70	2.17	1.03
L* = 60	2.70	1.25
L* = 50	3.10	1.47
L* = 40	3.37	1.68
L* = 30	3.16	1.83
Mean	2.68	1.34

TABLE VII. Comparison the Areas of Color Gamuts Obtainable in a Dye-Based IJ and a Photographic Color Paper Under D65 Illuminant and 2° Observer

Lightness	Dye-based IJ	Photo Color Paper
L* = 80	4948	3036
L* = 70	8947	5506
L* = 60	12266	7604
L* = 50	13582	8897
L* = 40	11203	9174
L* = 30	80980	8072
Mean	9654	7048

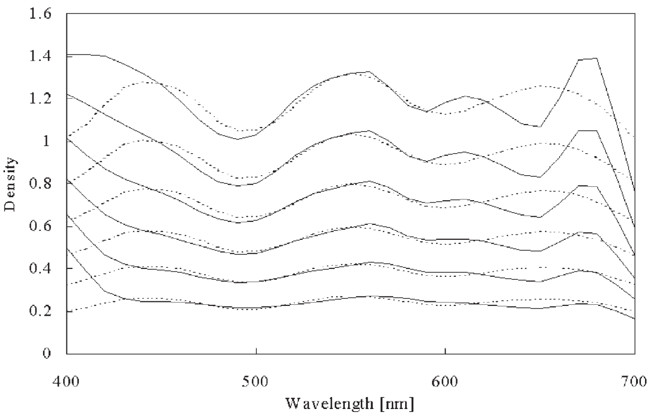

Figure 10. Spectral density of selective grays in a dye-based IJ (solid lines) and a photographic color paper (dotted lines).

Stability of gray balance was evaluated by metamerism index calculated as the CIE94 color difference under illuminant A for an estimated spectrum that resulted in a perfect colorimetric match under illuminant D65. Six lightness levels were probed where L* = 30, 40, 50, 60, 70, and 80. It can be seen in Fig. 10 that spectral densities of selective grays in a dye-based IJ exhibit more fluctuations than those in a photographic color paper. The combination of three dyes in a photographic color paper gives a selective gray that is more stable by about two-fold than that in a dye-based IJ as shown in Table VI.

Color Gamut

The areas of color gamuts obtainable by C, M, and Y dyes of Figs. 8 and 9 when they were used in a photographic color paper and in a dye-based IJ were calculated at six lightness levels of L* = 30, 40, 50, 60, 70, and 80 under D65 illuminant and 2° observer. It can be seen in Figs. 11 to 16 that the color gamut areas obtainable in a photographic color paper are smaller than those in a dye-based IJ. The latter is larger by about 1.4 times than the former as shown in Table VII.

The Effect of Ink Dilution

Stability of gray balance and obtainable color gamut[28] have been compared between the combination of C, M, and Y dyes and pC, pM, and Y dyes at three lightness levels of L* = 70, 80, and 90. Spectral reflection density curves of pC, pM, and Y dyes that are used in a dye-based IJ are shown in Fig. 17 after normalizing to 1.0 peak density.

Table VIII shows that the combination of pC, pM, and Y dyes gives a selective gray more than about three

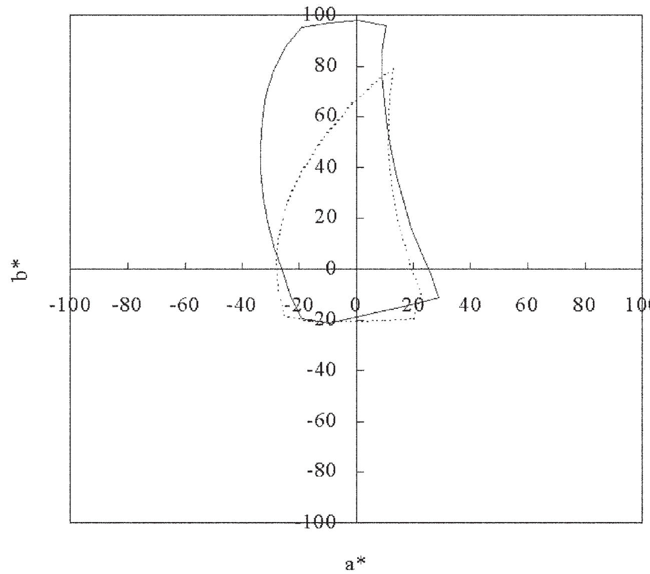

Figure 11. Color gamuts obtainable in a photographic color paper (dotted line) and a dye-based IJ (solid line) at L* = 80. (D65 illuminant, 2° observer)

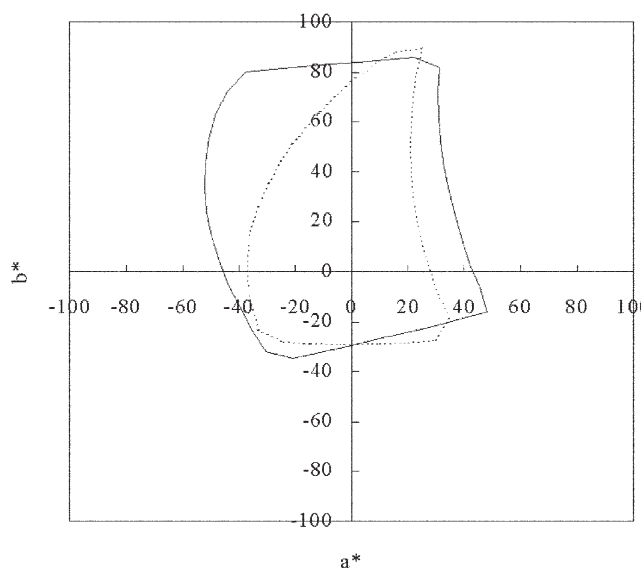

Figure 12. Color gamuts obtainable in a photographic color paper (dotted line) and a dye-based IJ (solid line) at L* = 70. (D65 illuminant, 2° observer)

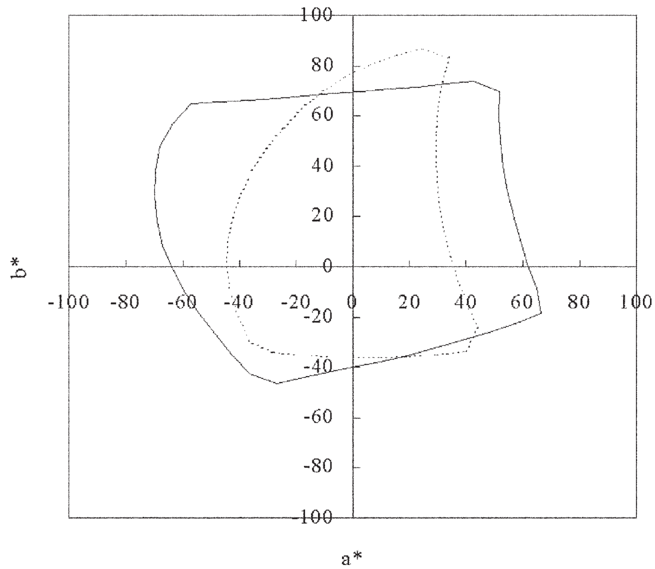

Figure 13. Color gamuts obtainable in a photographic color paper (dotted line) and a dye-based IJ (solid line) at L* = 60. (D65 illuminant, 2° observer)

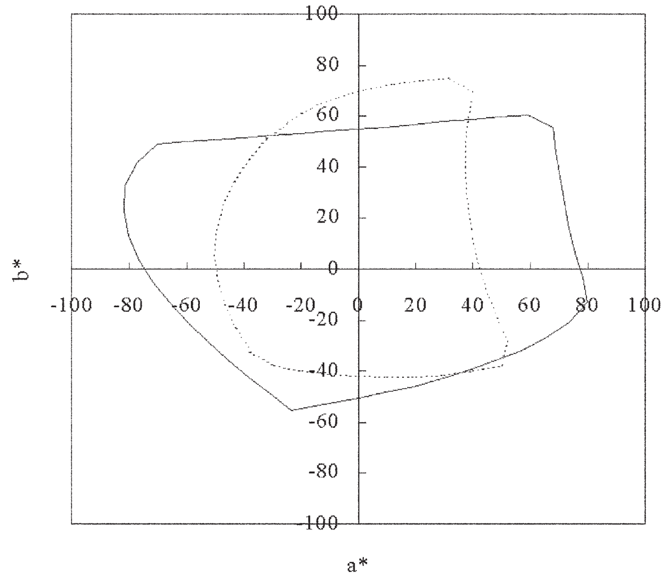

Figure 14. Color gamuts obtainable in a photographic color paper (dotted line) and a dye-based IJ (solid line) at L* = 50. (D65 illuminant, 2° observer)

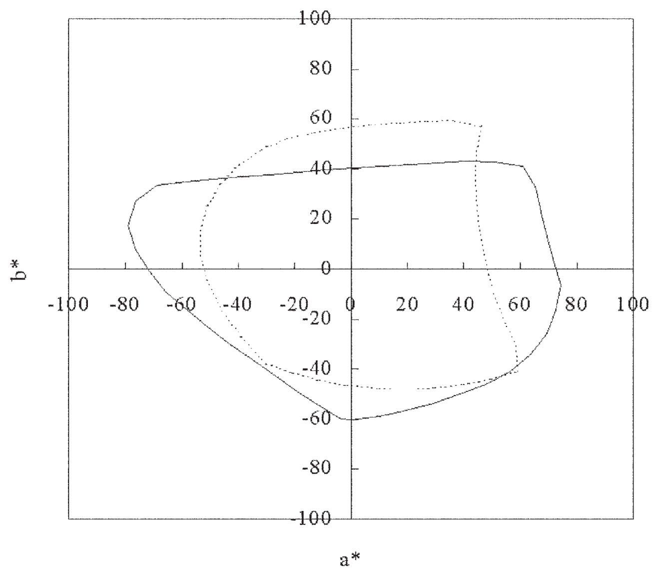

Figure 15. Color gamuts obtainable in a photographic color paper (dotted line) and a dye-based IJ (solid line) at L* = 40. (D65 illuminant, 2° observer)

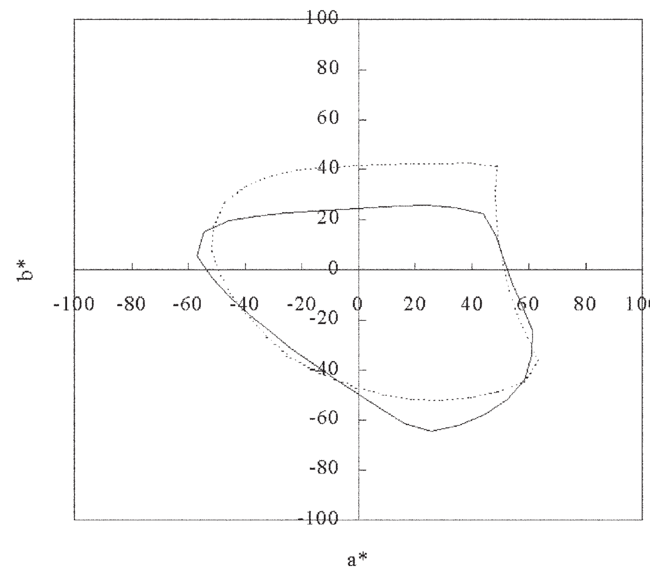

Figure 16. Color gamuts obtainable in a photographic color paper (dotted line) and a dye-based IJ (solid line) at L* = 30. (D65 illuminant, 2° observer)

TABLE VIII. Index of Metamerism Illuminant A

Lightness	pCpMY	CMY
L* = 90	0.36	0.69
L* = 80	0.52	1.58
L* = 70	0.64	2.17
Mean	0.51	1.48

TABLE IX. Comparison the Areas of Color Gamuts Obtainable by pC, pM, and Y Dyes and C, M, and Y Dyes

Lightness	pCpMY	CMY
L* = 90	948	901
L* = 80	5635	4948
L* = 70	9681	8947
Mean	5421	4932

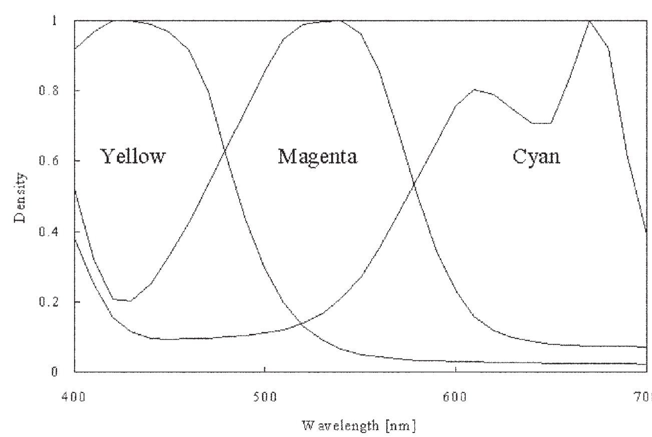

Figure 17. Spectral reflection density of pC, pM, and Y dyes for a dye-based IJ.

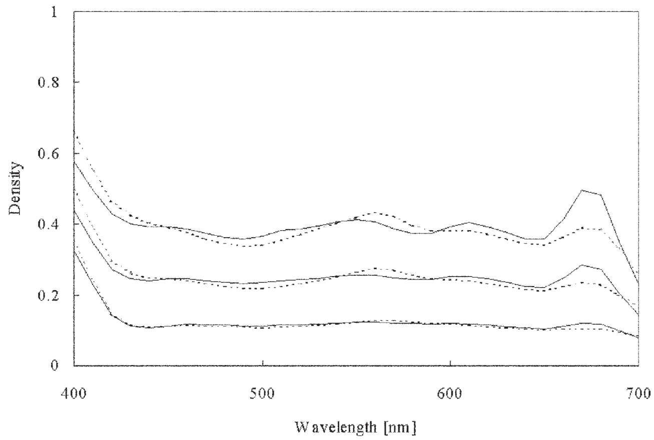

Figure 18. Spectral density of selective grays by the combination of pC, pM, and Y dyes (solid lines) and those of C, M, and Y dyes (dotted lines).

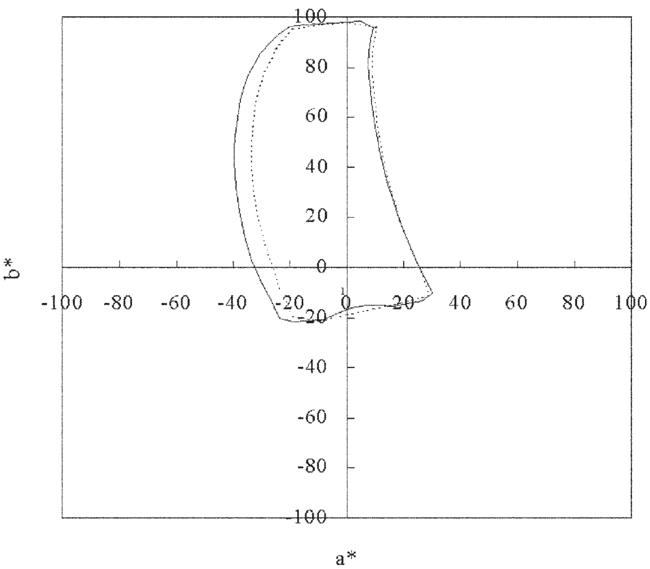

Figure 20. Color gamuts obtainable by pC, pM, and Y dyes (solid line) and by C, M, and Y dyes (dotted line) at L* = 80. (D65 illuminant, 2° observer).

times more stable than that of C, M, and Y dyes of IJ. However, it can be seen in Fig. 18 that spectral densities of selective grays by the combination of pC, pM, and Y dyes provided fluctuate more than those obtained by the combination of C, M, and Y dyes in the region above 650 nm. This is due to the spectral reflectance of pC dye.

It can be seen in Figs. 19 to 21 and Table IX that the areas of color gamuts obtainable by pC, pM, and Y dyes are larger by about 1.1 times than those from C, M, and Y dyes alone.

Conclusions

Five predicting models were compared for a dye-based IJ. Among these predicting models, only the CNM resulted in $\Delta E_{94} \cong 1.0$ when the set of primaries was 5^N (N is the number of colorants). However, this result is still inconvenient and unrealistic, because it is necessary to print and measure a lot of samples for prediction of reproduced tristimulus values. For example, six-colorant

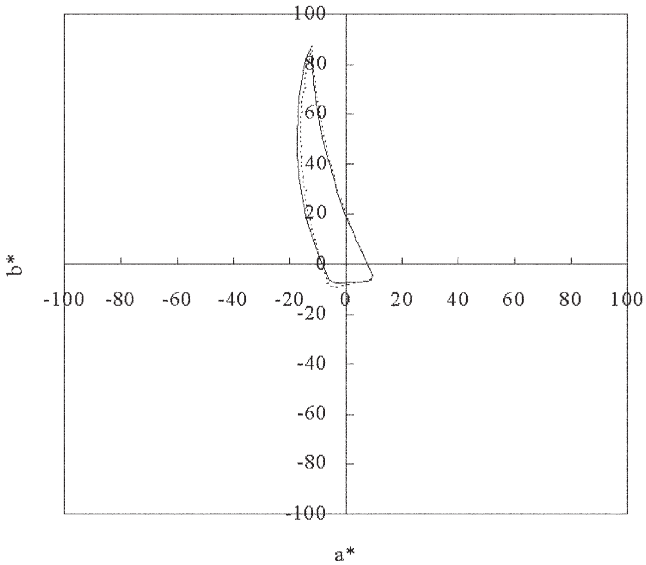

Figure 19. Color gamuts obtainable by pC, pM, and Y dyes (solid line) and by C, M, and Y dyes (dotted line) at L* = 90. (D65 illuminant, 2° observer).

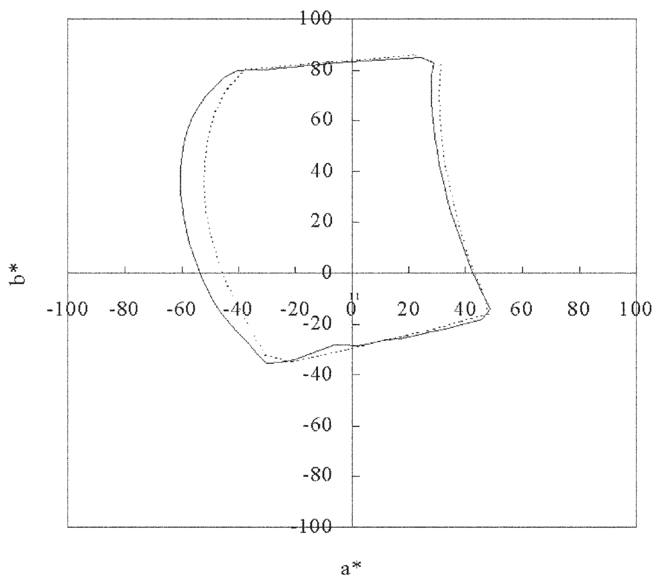

Figure 21. Color gamuts obtainable by pC, pM, and Y dyes (solid line) and by C, M, and Y dyes (dotted line) at L* = 70. (D65 illuminant, 2° observer).

prediction would require 15,625 = 5^6 primaries. Therefore, development of better predicting models that decrease the number of primaries while keeping good prediction accuracy will be necessary for dye-based IJ.

The areas of color gamuts obtainable in a dye-based IJ were larger by a factor of about 1.4 compared to those in a photographic color paper. For stability of gray balance, the combination of three dyes in a photographic color paper gave a selective gray about two-fold more stabler than that in a dye-based IJ. However, a dye-based IJ generally uses more than 4 inks, so a dye-based IJ can get a selective gray more stable than the combination of C, M, and, Y dyes.

Furthermore, the combination of pC, pM, and Y dyes produced a selective gray about three-fold more stabler than that of C, M, and Y dyes. The areas of color gamuts obtainable by pC, pM, and Y dyes are larger than those by C, M, and Y dyes by a factor of 1.1. Based on the above result, CMYKpCpM can be considered an effective system from the standpoint of color reproduction.

References

1. R. S. Berns, A. Bose and D, Tzeng, The spectral modeling of large-format inkjet printers, *RIT Munsell Color Science Laboratory Research and Development Final Report*, RIT, Rochester, NY, 1996.
2. R. Balasubramanian, Optimization of the spectral Neugebauer model for printer characterization, *J. Electron. Imaging* **8**(2), 156–166 (1999).
3. H. Kang, Applications of color mixing models to electronic printing, *J. Electron. Imaging* **3,** 276–287 (1994).
4. L. A. Taplin and R. S. Berns, Spectral color reproduction based on a six-color ink jet output system, *Proc. IS&T/SID 9th Color Imaging Conference*, IS&T, Springfield, VA, 2001, pp. 209–213.
5. N. Ohta, The color gamut obtainable by the combination of subtractive color dyes, *Photogr. Sci. Eng.* **15**(5), 399–422 (1971).
6. N. Ohta, The color gamut obtainable by the combination of subtractive color dyes, *Photogr. Sci. Eng.* **16**(3), 203–207 (1972).
7. N. Ohta, Stability of selective grey obtainable by use of subtractive colour dyes, *Photogr. Sci. Eng.* **20**(4), 149–153 (1972).
8. H. E. J. Neugebauer, Die theoretischen Grundlagen des Mehrfarbenedrückes, *Z. Wiss. Photog. Photophy. Photochem.* **36,** 73–89 (1937).
9. A. Murray, Monochrome reproduction in photoengraving, *J. Franklin Inst.* **221,** 721–744 (1936).
10. B. Kruse and S. Gustavson, Rendering of color on scattering media, *Proc. SPIE* **2657,** 422–431 (1996).
11. R. Balasubramanian, Colorimetric modeling of binary color printers, *Proc. IEEE International Conference on Image Processing*, vol. 2, IEEE Press, Los Alamitos, CA, 1995, pp. 327–330.
12. M. E. Demichel, *Le Proce'de'*, **26,** 17–21, 26–27 (1924).
13. J. A. S. Viggiano, The color of halftone tints, *Proc. TAGA*, 647–661 (1985).
14. J. A. S. Viggiano, Modeling the color of multi-color halftones, *Proc. TAGA*, 44–62 (1990).
15. J. A. C. Yule and W. J. Nielsen, The penetration of light into paper and its effect on halftone reproduction, *Proc. TAGA,* **4,** 66–75 (1951).
16. A. Beer, Bestimmung der absorption des rothen lichts in farbigen flussigkeiten, *Ann. Phys. Chem.* **86**(2), 78 (1852).
17. G. Wyszechki and W. S. Stiles, *Color Science Concepts and Methods, Quantitative Data and Formulae*, 2nd ed.. NY, John Wiley and Sons, New York, 1982, p. 30.
18. P. Kubelka and F. Munk, Ein Beitrag zur Optik der Farbenstriche, *Z. Tech. Phys.* **12,** 593–601 (1931).
19. H. R. Kang, Kubelka–Munk modeling of ink jet mixing, *J. Imaging Sci. Technol.* **17**(2), 76–83 (1992).
20. K. J. Heuberger, Z. M. Jing and S. Persiev, Color transformations and lookup tables, *Proc. TAGA/ISCC* **2,** 863–881(1992).
21. R. Rolleston and R. Balasubramanian, Accuracy of various types of Neugebauer models, *Proc. 1st IS&T/SID Color Imaging Conference*, IS&T, Springfield, VA, 1993, pp. 32–37.
22. A. U. Agar and J. P. Allebach, An iterative cellular YNSN method for color printer characterization, *Proc. 6th IS&T/SID Color Imaging Conference*, IS&T, Springfield, VA, 1998, pp. 197–200.
23. L. A. Taplin, *Spectral Modeling of a Six-Color Ink Jet Printer*, M.S. Thesis, Rochester Institute of Technology, Rochester, NY, 2001, pp. 3–8.
24. F. C. Williams and F. R. Clapper, Multiple internal reflections in photographic color prints, *J. Opt. Soc. Amer.* **43,** 595 (1953).
25. J. D. Shore and J. P. Spoonhower, Reflection density in photographic color prints generalizations of the Williams–Clapper transform, *J. Imaging Sci. Technol.* **45**(5), 484–488 (2001).
26. J. A. C. Yule, *Principles of Color Reproduction*, John Wiley and Sons Inc., New York, 1967, p. 209.
27. N. Ohta, Reflection density of multilayer color prints, *Photogr. Sci. Eng.* **15**(6), 487–494 (1971).
28. E. Baumann and R. Hofmann, Colour aspects in photo-quality ink-jet printing, *IS&T Reporter* **17**(3), 1–4 (2002).